Polymer Degradation and Stability 96 (2011) 1761–1770

Contents lists available at ScienceDirect

Polymer Degradation and Stability

journal homepage: www.elsevier.com/locate/polydegstab

Impact of formic/acetic acid and ammonia pre-treatments on chemical structure and physico-chemical properties of *Miscanthus x giganteus* lignins

Caroline Vanderghem [a,b,*,1], Aurore Richel [a,1], Nicolas Jacquet [a,b], Christophe Blecker [b], Michel Paquot [a]

[a] Department of Industrial Biological Chemistry, Gembloux Agro Bio-Tech, University of Liège, Passage des Déportés 2, B-5030 Gembloux, Belgium
[b] Department of Bioresources Valorisation, Gembloux Agro Bio-Tech, University of Liège, Passage des Déportés 2, B-5030 Gembloux, Belgium

A R T I C L E I N F O

Article history:
Received 12 May 2011
Accepted 28 July 2011
Available online 5 August 2011

Keywords:
Miscanthus x giganteus
Ammonia pretreatment
Formic/acetic acid pretreatment
Lignin chemical structure
Lignin characterisation
Repolymerisation

A B S T R A C T

Miscanthus x giganteus was treated with formic acid/acetic acid/water (30/50/20 v/v) for 3 h at 107 °C and 80 °C, and soaking in aqueous ammonia (25% w/w) for 6 h at 60 °C. The effects of these fractionation processes on chemical structure, physico-chemical properties and antioxidant activity of extracted lignins were investigated. Lignins were characterized by their purity, carbohydrate composition, thermal stability, molecular weight and by Fourier transform infrared (FTIR), 1H and quantitative 13C nuclear magnetic resonance (NMR), adiabatic broadband {13C–1H} 2D heteronuclear (multiplicity edited) single quantum coherence (g-HSQCAD). The radical scavenging activity towards 2,2-diphenyl-1-picrylhydrazyl (DPPH) was also investigated. Formic/acetic acid pretreatment performed in milder conditions (80 °C for 3 h) gave a delignification percentage of 44.7% and soaking in aqueous ammonia 36.3%.

Formic/acetic acid pretreatment performed in harsh conditions (107 °C for 3 h) was more effective for extensive delignification (86.5%) and delivered the most pure lignin (80%). The three lignin fractions contained carbohydrate in different extent: 3% for the lignin obtained after the formic/acetic acid pretreatment performed at 107 °C (FAL-107), 5.8% for the formic/acetic acid performed at 80 °C (FAL-80) and 13.7% for the ammonia lignin (AL). The acid pretreatment in harsh conditions (FAL-107) resulted in cleavage of β–O-4′ bonds and aromatic C–C. Repolymerisation was thought to originate from formation of new aromatic C–O linkages. Under milder conditions (FAL-80) less β–O-4′ linkages were broken and repolymerisation took place to a lesser extent. Ammonia lignin was not degraded to a significant extent and resulted in the highest weight average 3140 g mol^{-1}. Despite the fact of FAL-107 repolymerisation, significant phenolic hydroxyls remained free, explaining the greater antioxidant activity.

© 2011 Elsevier Ltd. All rights reserved.

1. Introduction

Lignin constitutes 15–30% by weight of the lignocellulosic biomass [1], and after cellulose and hemicellulose it is the third most abundant biopolymer on earth. This major cell wall component fills the spaces between cellulose, hemicellulose and pectin and crosslinks polysaccharides conferring the strength and rigidity of the lignocellulose matrix. In addition, lignin polymer conducts water and nutrients in stems and protects the cell wall from microorganism attacks [2].

This complex three-dimensional amorphous polymer is composed of methoxylated phenylpropane structures and their precursors are three aromatic alcohols namely *p*-coumaryl, coniferyl and sinapyl alcohols. These molignols are incorporated into lignin in the form of *p*-hydroxyphenyl (H), guaiacyl (G), and syringyl (S) respectively [3]. Depending on their origin (hardwoods, softwoods, grasses), the type of monolignols units differs. Lignins from woods are mainly composed of guaiacyl and syringyl, whereas herbaceous plants contain all the three units (H, G, S) [2]. Different types of linkages connect the phenylpropane units, where the most common is the β–O-4′ linkage consisting of more than half of the lignin linkages [4]. Lignin is linked to the other polymers through covalent bonds: α-ether, α-ester [5,6] and phenyl glycosidic linkages [7].

Despite the fact that lignin is the major aromatic bio-resource, it has received less attention with regards to value enhancement compared to cellulose. From the pulp and paper industry, only 2% of the lignins are used for commercial purposes [8]. With its aromatic structure and chemical properties a wide variety of bulk and fine chemicals can be produced in a sustainable way and may substitute petroleum based compounds. Biofuels or bulk aromatic

---

* Corresponding author. Department of Industrial Biological Chemistry, Gembloux Agro Bio-Tech, University of Liège, Passage des Déportés 2, B-5030 Gembloux, Belgium. Tel.: +32 81 62 22 32; fax: +32 81 62 22 31.

E-mail addresses: cvanderghem@ulg.ac.be (C. Vanderghem), a.richel@ulg.ac.be (A. Richel).

[1] Both authors contributed equally to this study.

0141-3910/$ – see front matter © 2011 Elsevier Ltd. All rights reserved.
doi:10.1016/j.polymdegradstab.2011.07.022

and phenolic compounds can be produced by catalytic lignin conversion, (hydro)cracking or lignin reduction reactions. Lignin oxidation reactions are used to make functionalized aromatics for the production of fine chemicals. High molecular weight lignin can be used to produce carbon fibres, polymer modifiers, adhesives, and resins [9]. In addition, lignins have antioxidant activity due to their diverse functional groups (phenolic groups, hydroxyl groups, …) [10].

A growing number of environmental friendly fractionation technologies to remove lignin from the lignocellulose are being developed, and each method changes the lignin form and chemical properties to a greater or lesser extent. No one method is ideal and the advantages and limitations of each method have to be evaluated in terms of the overall valorization of the lignocellulose material.

Miscanthus x giganteus, which can grows 4 m high and gives high yields of biomass per hectare, was identified as a potential high-yielding bioenergy crop in Europe and the USA number of treatments have been applied on *Miscanthus x giganteus* in order to delignify it for pulp production, before enzymatic saccharification or for lignin isolation [11–15].

In this study, the effect of different fractionation processes on chemical structure, physico-chemical properties and antioxidant activity of *Miscanthus x giganteus* lignin were investigated. Three different lignin preparations were obtained by: (i) formic/acetic acid pretreatment under harsh conditions, (ii) formic/acetic acid pretreatment under mild conditions, (iii) soaking in aqueous ammonia. Extracted lignins were subjected to characterisation by FTIR, TGA, ^{1}H NMR, quantitative ^{13}C NMR, g-HSQCAD NMR and gel permeation chromatography in order to investigate the effect of the pre-treatments on the chemical structure and physico-chemical characteristic. The radical scavenging activity towards 2,2-diphenyl-1-picrylhydrazyl (DPPH) was also investigated.

2. Material and methods

2.1. Raw material

Miscanthus x giganteus comes from a crop cultivated in spring 2007, and harvested after two years (Tournai, Belgium). Stems were stripped of leaves, air dried and ensiled. The material was ground to particles around 1–2 mm. The untreated miscanthus was mainly composed of 24.5% lignin, 48.4% glucose, 15.7% xylose, 1.9% arabinose, 1.2% galactose, 0.2% mannose, 6.4% extractives and 2.4% ash.

2.2. Formic/acetic acid pretreatment

Miscanthus x giganteus was pre-treated by the protocol described in Lam et al. [16] with some modifications. Pre-treatments were performed in 500 mL double-necked boiling flasks and heated by heating plates. First, the material was soaked at 50 °C for 30 min in a formic acid/acetic acid/water mixture (30/50/20 volume ratio) at a liquid/dry matter of 25/1. After soaking, the temperature and time of cooking was set to 107 °C for 3 h for the harsh conditions and 80 °C for 3 h for the mild conditions. During cooking, stirring was continuously performed with a stir bar at 450 rpm. After heating, reactions were stopped by removing the flasks from the heating plates, and allowed to cool at room temperature. The pulps were filtered with a vacuum filter funnel (500 mL, 95 mm diameter) assembled with a fritted disk (40–100 μm pore size; Robu Glasfilter–Geräte GmbH). Vacuum was run until black liquor was no longer being collected. Following filtration, pulps were washed twice with the same cooking mixture. The liquor and washes were combined and 9 volumes of water were added with stirring in order to precipitate the lignins (around pH 2). Lignins were recuperated after centrifugation, washed with acidified water, vacuum filtered (fritted disk 1–1.5 μm pore size) and freeze-dried. Extractions were performed in duplicate.

2.3. Soaking in aqueous ammonia pretreatment

Ammonia pretreatment was performed in 1L Duran bottles. The raw material was soaked in aqueous ammonia (25% w/w) at a liquid/dry matter of 12/1, at 60 °C during 6 h in a water bath. After soaking, the bottles were removed from the water bath, and allowed to cool at room temperature. The pulps were filtered with a vacuum filter funnel (500 mL, 95 mm diameter) assembled with a fritted disk (40–100 μm pore size; Robu Glasfilter-Geräte GmbH). Vacuum was run until black liquor was no longer being collected. Following filtration, pulps were washed twice with distilled water at a liquid/initial dry matter of 10/1. The liquor and washes were combined and ammonia was vacuum-evaporated at 40 °C. Lignins in the liquor were precipitated by addition of sulphuric acid (72% w/w) until a pH of 2 was reached. Lignins were recuperated after centrifugation, washed with acidified water, vacuum filtered (fritted disk 1–1.6 μm pore size) and freeze-dried. Extractions were performed in duplicate.

2.4. Composition of the isolated lignins

Klason lignin was determined according to the procedure described in Sluiter et al. [17].

Monosaccharides were determined as alditol acetates by gas chromatography according to the procedure described in Blakeney et al. [18]. Analyses were carried out with a Hewlett–Packard (HP 6890) gas chromatograph equipped with a flame ionization detector. The components were separated using a high performance capillary column, HP1-methylsiloxane (30 cm × 320 μm, 0.25 μm, Scientific Glass Engineering, S.G.E. Pty. Ltd., Melbourne, Australia). Data were analyzed using ChemHP software. 2-Deoxyglucose (internal standard), glucose, xylose, arabinose, mannose and galactose were obtained from Sigma–Aldrich (St-Louis, USA), solutions of known concentrations were used as standards. Analyses were performed in duplicate.

2.5. Thermogravimetric analysis

Thermogravimetric analyses were performed on a TGA analyzer unit (Mettler Toledo) under a flowing nitrogen atmosphere. Approximately 10 mg of sample was heated in a porcelain crucible up to 800 °C at a rate of 10 °C/min. Analyses were performed in duplicate.

2.6. Infrared spectroscopy

About 5 mg of dried lignin were mixed and ground with potassium bromide and then mechanically pressed in order to form a pellet. FTIR spectra were recorded in the 2000–400 cm^{-1} range with 16 scans at a resolution of 4 cm^{-1} on a Bruker IFS 48 spectrometer.

2.7. Acetylation of lignins

Approximately 50 mg of lignins were stirred in 1 mL of acetic anhydride/pyridine (1:1, v/v) at room temperature for 24 h. The solution was diluted with 30 mL ethanol and stirred for 30 min, and then removed with a rotary evaporator. This operation was repeated 4 times to ensure removal of the solvents. The acetylated lignins were dissolved in 10 mL chloroform, washed twice with deionised water and dried with anhydrous sodium sulphate. The acetylated lignins in the chloroform were added drop-wise to 150 mL of diethyl ether. The acetylated lignins (precipitate) were recuperated and air-dried then dried under vacuum at 40 °C.

2.8. NMR spectroscopy

NMR analyses were performed using a Varian Unity 600 MHz instrument at 298 K. Around 75 mg of lignin were dissolved in 0.75 ml DMSO-d_6. Chemical shifts were referenced to TMS (0.0 ppm). ^{1}H NMR spectra were recorded with a 45° observed pulse width and a 1.704 s acquisition time. A total of 128 scans were collected. Adiabatic broadband {^{13}C-^{1}H} 2D heteronuclear (multiplicity edited) single quantum coherence (g-HSQCAD) analyses were performed applying a Varian ChemPack 4.0 pulse sequence with 2048 collected complex points for the ^{1}H dimension and with a relaxation delay of 5 s. The number of transients was 32, and 256 time increments were recorded in the ^{13}C dimension. The $^1J_{C-H}$ used was 140 Hz. Gauss apodisation function was applied in both dimensions. For quantitative ^{13}C NMR, a 90° pulse width, a 1.4 s acquisition time, and a 1.7 s relaxation delay were applied. Chromium(III) acetylacetonate (0.01 M) was added to lignin samples to ensure complete relaxation of all nuclei. A total of 40 000 scans were collected.

Samples of acetylated lignins were dissolved in DMSO-d_6 (at the approximate concentration of 50 mg in 0.25 ml). NMR analyses were performed using a 5 mm Shigemi NMR microtube, with the susceptibility matched to dimethylsulfoxide. g-HSQCAD spectra were collected under the same conditions as above.

2.9. Size exclusion chromatography

Samples molecular weights were determined by gel permeation chromatography (GPC) after acetylation of lignins to allow dissolution in tetrahydrofuran (THF). Three Styragel columns (HR1, HR2 and HR3) (Waters) were connected in series to an HPLC system (Agilent Technologies, 1200 series) equipped with a differential refractometer (BI-DNDC/GPC, 620 nm). The acetylated lignins were dissolved in THF at the concentration of 1 mg/mL and the solution was filtered through a 0.45 μm filter. 100 μl were injected into the HPLC system and THF was used as the eluent with a flow rate of 1 mL/min. Calibration curve was constructed with polystyrene standards (Sigma–Aldrich). Analyses were performed in duplicate.

2.10. Evaluation of lignin antioxidant activity

The antioxidant activity of the isolated lignins was performed using the spectrophotometric procedure based on the use the free radical 2,2-diphenyl-1-picrylhydrazyl (DPPH) described in Dizhbite et al. [10]. Lignin samples were dissolved in dioxane/water (90:10, v/v) at different concentrations. 0.1 ml of lignin sample solution was mixed with 3.9 ml of a 6×10^{-5} mol/L DPPH solution and the absorbance of the mixture was immediately measured using a Ultrospect 4000 (Pharmacia BioTech) spectrophotometer. The decrease in absorbance was measured every 5 s, until the steady state was reached. The percentage of DDPH remaining at the steady state was plotted as a function of the lignin concentration. From this graph the lignin concentration needed to decrease the initial DPPH concentration by 50% was determined and was defined as EC_{50}. Radical scavenging index (RSI) was defined as the inverse of EC_{50}. Analyses were performed in duplicate.

3. Results and discussion

3.1. Composition of the isolated lignins

Depending on the conditions of the pre-treatments, different delignification degrees were obtained on the pulps. The pretreatment that gave an extensive delignification (86.5%) was the formic/acetic acid performed at 107 °C for 3 h. The second formic/acetic acid pretreatment achieved in milder conditions (80 °C for 3 h) gave almost the half delignification value (44.7%). A smaller delignification value was obtained with the ammonia pretreatment (36.3%). The largest delignification value can be explained by the harshness temperature conditions allowing more lignin to solubilise.

Table 1 shows the lignin content determined by the Klason procedure and the monosaccharide composition of the isolated fractions. The lignin purity of the three different fractions were of: 80% for the lignin obtained after the formic/acetic acid pretreatment performed at 107 °C (FAL-107), 68% for the formic/acetic acid performed at 80 °C (FAL-80) and 70% for the ammonia lignin (AL). Lignin obtained in the harshness condition was more pure probably due to a dissociation of carbohydrate in the lignin fraction.

Carbohydrate content for FAL-107, FAL-80 and AL was of 3%, 5.8% and 13.7% respectively. A clear effect of pretreatment conditions on the amount of carbohydrates was observed. The pretreatment for to obtain FAL-107 resulted in intensive hydrolysis of lignin-carbohydrates bonds resulting in low carbohydrate content in the isolated lignin. The main hemicelluloses bonded to this lignin were xylan and arabinan. Glucose and galactose were also present but in a minor amount. Mannose was present in trace amount. FAL-80 resulted in higher carbohydrate content as a result of the milder conditions of the pretreatment. AL preparation had a noticeable amount of xylan. This suggests that xylose may link to lignin by bonds that are resistant to cleavage under the ammonia conditions used in this work.

3.2. Thermogravimetric analysis

Fig. 1 shows the thermogravimetry (TG) curves, where the weight loss of lignins is plotted in relation to the temperature of thermal degradation (Fig. 1a), and the first derivatives of this curve (weight loss rate) is known as differential thermogravimetry (DTG) (Fig. 1b). Three stages of decomposition can be clearly identified in the TG curves for the three lignins (FAL-107, FAL-80 and AL). In the

Table 1
Carbohydrate and lignin analysis of formic/acetic acid lignins FAL-80, FAL-107, and ammonia lignin AL isolated from *Miscanthus x giganteus*.

Sample	Klason lignin(%)	Pentoses		Hexoses		
		Arabinose(%)	Xylose	Mannose(%)	Galactose(%)	Glucose(%)
FAL-107	80	1.2	1.1	0.1	0.2	0.4
FAL-80	68	0.6	2.8	0.2	0.3	1.9
AL	70	1.9	10.8	0.1	0.3	0.6

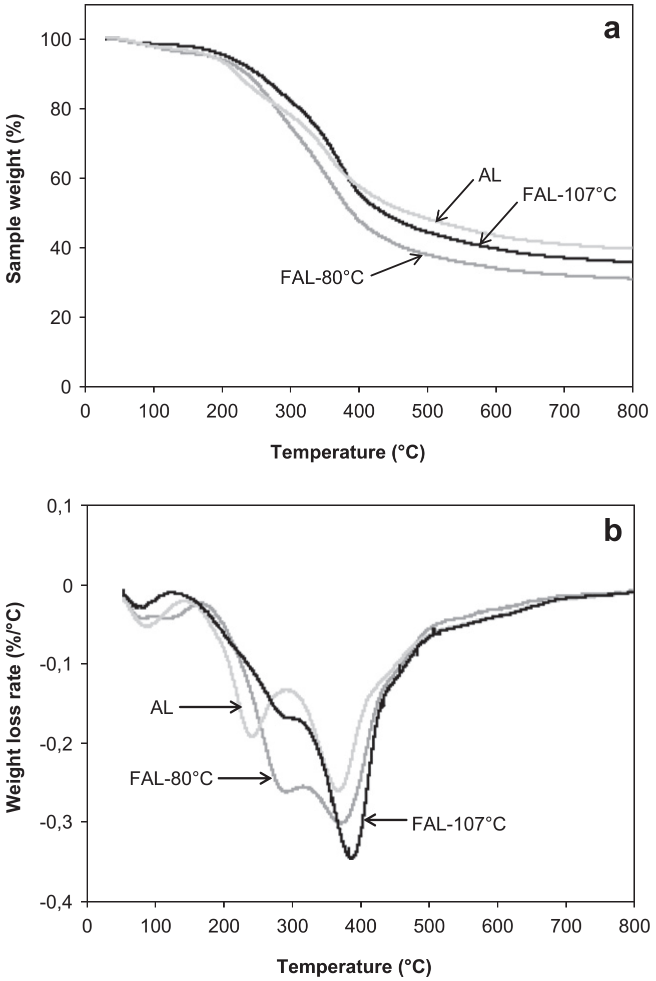

Fig. 1. TG (a) and DTG curves (b) of formic/acetic acid lignins FAL-80, FAL-107, and ammonia lignin AL isolated from *Miscanthus x giganteus*.

first stage, temperature below 200 °C, the weight loss of the three materials were less than 7% and corresponds to the evaporation of light volatiles (mainly water). The second stage of decomposition, occurring between 200 and 500 °C, corresponds to a remarkable drop in weight of samples (38–48%) due to liberation of volatile hydrocarbon from rapid thermal decomposition of hemicelluloses, cellulose and some part of lignins. The third stage, after 500 °C, the weight loss is less important than the second period due to the steady decomposition of the more heavy components mainly from lignin [19].

The isolated lignins exhibited different DTG profiles. The first peak for the three lignins ranged from 40 to 125 °C and corresponded to the gradual evaporation of the moisture. For FAL-107 a second large peak could be observed from approximately 125 °C–700 °C ($DTG_{max} = 387$ °C), with a shoulder at 293 °C. FAL-80 showed a similar profile but with a great weight loss rate around 293 °C. AL showed a double-peak distribution, where the first peak started from 150 °C to 300 °C ($DTG_{max} = 240$ °C), and the second peak from 300 °C to 700 °C ($DTG_{max} = 372$ °C). According to Wu et al. [20], hemicellulose is the most reactive compound which decomposes at between 200 and 350 °C. Lignin is more thermally stable and decomposes between 250 and 500 °C. However some studies reported that pyrolysis of lignin can occur as low as 150 up to 900 °C [21]. The regions between 150 °C and 300 °C could mainly be attributed to the decomposition of hemicellulose, but an overlap with lignin cannot be excluded. The peaks between 300 and 700 °C could mainly correspond to lignin decomposition. FAL-80 and AL presented more important peaks in the region of the hemicelluloses confirming the carbohydrate analysis. Carbohydrate linkages in FAL-107 were further cleaved compared to FAL-80 and AL.

3.3. *Infrared spectroscopy analysis*

The FTIR spectra of FAL-107, FAL-80 and AL are shown in Fig. 2, and Table 2 gives the signal assignments compared to previously published data on lignin [13,15,22,23].

The bands between 1790 and 1680 cm^{-1} are characteristic of carbonyls. The bands at 1709 cm^{-1} and 1690 cm^{-1}, observed in AL, were assigned to non conjugated carbonyl groups and conjugated carbonyl groups respectively. The bands around 1604, 1515 and 1424 cm^{-1} in all the lignins, are characteristic of aromatic ring vibrations of the phenylpropane groups. Absorptions at the wavelengths of 1330, 1124 cm^{-1}corresponded to syringyl units and those around 1268, 1161 cm^{-1} to guaiacyl units.

Despite some differences, FAL-107, FAL-80 and AL spectra profiles are globally rather similar, indicating a comparable chemical structure of the extracted lignins. A major difference can be observed in the carbonyl region (1760 and 1650 cm^{-1}), where the band of FAL-107 and FAL-80 had a greater relative intensity compared to AL. The acid hydrolysis of lignin could have generated new carbonyl groups [22]. In addition, the carbonyl group of residual acetic acid in FAL lignin could have increased the intensity. A relative slighter higher intensity between 700 and 500 cm^{-1} in AL and FAL-80 could have corresponded to carbohydrates.

3.4. *NMR spectroscopy analysis of nonacetylated lignins*

The main structural features of nonacetylated lignin preparations, including major units linked by ether, ester and C—C bonds, were revealed by ^{1}H and ^{13}C NMR in combination with two-dimensional $\{^{13}C–^{1}H\}$ HSQC technique.

The assignment of the signals from ^{1}H, ^{13}C and HSQC spectra was achieved on the basis of the lignin NMR database and descriptive literature (Tables 3–5) [12,24,25].

Classical ^{1}H experiments were performed to elucidate roughly the chemical structure of the different lignin samples (Fig. 3). The

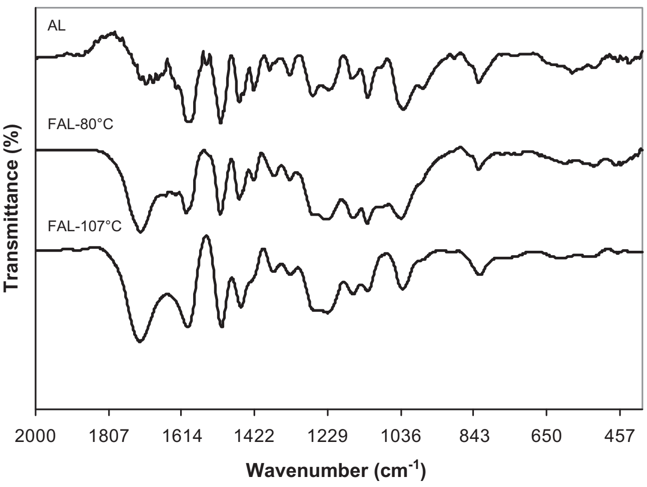

Fig. 2. FTIR spectra of formic/acetic acid lignins FAL-80, FAL-107, and ammonia lignin AL isolated from *Miscanthus x giganteus*.

Table 2
Signal assignment in FTIR spectra of formic/acetic acid lignins FAL-80, FAL-107, and ammonia lignin AL isolated from *Miscanthus x giganteus*.

FAL-107 FAL-80 (Peak cm^{-1})	AL Peak (cm^{-1})	Assignment	Values in literature (Peak cm^{-1})
1790–1680	1790–1680	Acetate carbonyl group	1739[a]
		p-coumaryl ester group (carbonyl group resonance)	1705[a]
		Non conjugated carbonyl groups	1705[b]
		Conjugated carbonyl groups	1698[c]
1604	1597	Aromatic ring vibrations of the phenylpropane groups	1600[b]
		Aromatic skeleton vibrations, C–C bounds	1604[c]
1515	1513	Aromatic skeleton vibrations, C–C bounds	1512[c]
		Aromatic ring vibrations of the phenylpropane groups	1515[b]
1463	1463	C–H vibration of CH_2 and CH_3 groups	1460[b]
		C–H deformations and aromatic ring vibrations	1464[c]
1424	1424	Aromatic skeleton vibrations, C–C bounds	1422[c]
		Aromatic ring vibrations of the phenylpropane groups	1425[b]
1330	1329	Syringyl units	1330[c]
		Syringyl units with C–O stretching	1330[b]
1268	1267	G units aromatic ring	1263[d]
		Guaiacyl units	1265[b]
1220	1220	Syringyl and guaiacyl ring breathing with C–O stretching	1218[b]
		Ether group vibration	1220[b]
1161	1161	Guaiacyl units	1153[c]
1124	1125	Syringyl units	1120[c]
		Syringyl units with C–O stretching	1120[b]
		Syringyl type aromatic C–H in plane deformations	1125[b]
1031	1030	Aromatic and aliphatic OH groups	1030[b]
		Aromatic in plane G unit	1034[d]
		Guaiacyl units	1037[c]
832	833	Syringyl band	825[b]
		Out of plane C–H bending S	835[d]

[a] El Hage et al. [13].
[b] Serrano et al. [22].
[c] Sun et al. [23].
[d] Villaverde et al. [15].

Table 3
Signals assignment in ^{13}C and g-HSQCAD NMR spectra of ammonia lignin. Results for quantification of functional groups on the basis of ^{13}C NMR data collected in the presence of $Cr(acac)_3$ as the spin relaxing agent (0.01M).

Labels	δ ^1H (ppm)	δ ^{13}C (ppm)	Assignment	Value (per Ar)[a]
1	–	166.9	C_γ in etherified ferulic acid	0.06
2	–	160.3	C_4 in esterified *p*-coumaric acid	
3	–	153.1–152.6	C_3, C_5 in etherified syringyl units	0.73
4	–	150.0	C_3 in etherified guaiacyl units	0.31
5	–	147.9	C_3, C_5 in non etherified syringyl units	
6	–	147.5	C_4 in etherified guaiacyl units	
7	7.40	145.8	}C_α in etherified ferulic acid	
	7.44	144.8		
8	7.28	139.7	*n.a*	
9	7.44	130.7	C_2, C_6 in esterified *p*-coumaric acid	0.21
10	–	125.4	C_1 in esterified *p*-coumaric acid	0.12
11	6.44	120.5	*n.a.*	
12	6.74	119.5	C_6 in guaiacyl units	
13	6.75 (H_3)	117.8	}C_3, C_5 in esterified *p*-coumaric acid	0.21
	6.75 (H_5)	116.2		
14	6.92	115.7	}C_β, C_5 in etherified ferulic acid	
15	6.66	115.2		
16	6.23	114.3	C_5 in guaiacyl units	
17	6.96	111.6	C_2 in guaiacyl units	
18	6.66	104.3	}C_2, C_6 in syringyl units	
	6.61	103.8		
19	–	102.2	*n.a.*	
20	4.07	86.5	C_β in β–O-4′ linked to an S unit	
21	4.24	84.4	C_β in β–O-4′ linked to a G unit	
–	3.79	80.7	}Carbohydrate contamination	
–	3.48	75.9		
–	3.23	74.4		
–	3.01	73.1		
22	4.78	72.4	C_α in β–O-4′ linkages	0.43
23	3.85[b]	63.6	}C_γ in β–O-4, with $C_\alpha = O$	
	3.14[b]	63.6		
24	3.68[b]	63.3	C_γ in phenylcoumaran substructures	
25	3.43[b]	62.3	C_γ in cinnamyl (sinapyl/coniferyl) alcohol end-groups	
26	4.05[b]	62.0		
27	3.19[b] (γ_1)	60.4	}C_γ in β–O-4′ linkages	0.31
	3.58[b] (γ_2)	60.4		
28	3.69	56.2	$-OCH_3$ in syringyl and guaiacyl units	0.98

n.a. stands for "not assigned".
[a] Integral value for structural moieties expressed per one aromatic ring. The integral between 162-102 ppm was set as the reference, assuming that it represents 6.12 aromatic carbons (all aromatic C + a contribution of 0.12 from the unsaturated side chains of coumaric and coniferic groups).
[b] Protons referred to CH_2 in the HSQC spectrum.

oxygenated aliphatic region of the ^1H spectra for both formic/acetic acid (FAL-107 and FAL-80) and ammonia (AL) pre-treated lignins clearly evidenced the methoxy substituents of constitutive aromatic monolignols at $\delta_H \sim 3.6–3.7$ ppm. Between 6.0 and 7.5, the area was related to aromatic protons, and protons in aliphatic groups were detected between $\delta_H \sim 0.5–2.0$ ppm. Signals around 4.2–5.0 ppm, observed mainly in ammonia lignin, were notably typical of protons in inter-unit ether structures, validating at first sight a more polymerised material [26].

3.5. Characterisation of lignins by 2D correlation NMR

A more accurate description of the composition of the different lignin fractions was proposed using 2D correlation {^{13}C–^1H} HSQC technique. Three main regions were depicted corresponding to aliphatic (δ_C/δ_H 10–50/0.5–2.0), side-chain (δ_C/δ_H 50–90/2.5–5.5) and aromatic (δ_C/δ_H 95–160/5.5–8.0) ^{13}C–^1H correlations. The (non-oxygenated) aliphatic area displayed signals with poor structural information (especially methoxy substituents and alkyl chains) and was not herein discussed in details.

The S:G:H distribution in lignins is classically visualised in the two-dimensional aromatic area of the {^{13}C–^1H} HSQC spectra between δ_C/δ_H 104–125/6.0–6.8. The aromatic section of our lignin samples suggested normal presence of syringyl and guaiacyl rings, as previously highlighted by FTIR measurements. Syringyl units displayed specific strong cross-signals δ_C/δ_H 104.3/6.66 ($C_{2,6}$–$H_{2,6}$ correlations), while guaiacyl moieties showed different specific resonances at δ_C/δ_H 119.5/6.74–114.3/6.23 and 111.6/6.96 (respectively C_6–H_6, C_5–H_5 and C_2–H_2 correlations) (Fig. 4). In complement, signals for *p*-coumarate structures were observed by very predominant aromatic ring cross-signals at δ_C/δ_H 130.7/7.44 (C_2 and C_6) and 116.2/6.75 (C_3 and C_5). These *p*-coumaric acid esters are typical of *Miscanthus x giganteus* lignin skeleton [15]. The signal at δ_C/δ_H 145.5/7.40 was attributed to C_α–H_α correlation and was related to the occurrence of etherified ferulic acid structures.

For ammonia lignin, in the oxygenated side-chain area of the HSQC spectrum (Fig. 5a), the presence of classical predominant β–O-4′ and phenylcoumaran lignin substructures were identified at notably δ_C/δ_H 72.4/4.78 for CH_α in β–O-4′ and δ_C/δ_H 63.3/3.68 for

Table 4

Signals assignment in ^{13}C and g-HSQCAD NMR spectra of formic/acetic acid lignin. Results for quantification of functional groups on the basis of ^{13}C NMR data collected in the presence of $Cr(acac)_3$ as the spin relaxing agent (0.01M).

Labels	δ ^1H (ppm)	δ ^{13}C (ppm)	Assignment	Value (per Ar)[a]
29	–	172.5	Aliphatic COOR	
30	–	170.5	$OC(O)CH_3$	
1	–	166.9	C_γ in etherified ferulic acid	0.18
2	–	160.3	C_4 in esterified *p*-coumaric acid	
3	–	153.1–152.6	C_3,C_5 in etherified syringyl units	0.31
4	–	150.0	C_3 in etherified guaiacyl units	0.37
5	–	147.9	C_3,C_5 in non etherified syringyl units	
6	–	147.5	C_4 in etherified guaiacyl units	
7	7.40	145.8	C_α in etherified ferulic acid	
9	7.44	130.7	C_2,C_6 in esterified *p*-coumaric acid	0.61
10	–	125.4	C_1 in esterified *p*-coumaric acid	0.18
12	6.74	119.5	C_6 in guaiacyl units	
13	6.75 (H_5)	116.2	C_3, C_5 in esterified *p*-coumaric acid	0.61
16	6.23	114.3	C_5 in guaiacyl units	
17	6.96	111.6	C_2 in guaiacyl units	
18	6.66	104.3	C_2, C_6 in syringyl units	
19	–	102.5	*n.a.*	
31	3.71	83.1	Polysaccharide contamination	
32	4.49	81.1	*n.a.*	
33	3.98	80.0	Polysaccharide contamination (carbohydrate–lignin complexes)	
	3.63	77.5		
	4.75	71.7		
34	4.24[b]	65.2	}Cγ in β–5substructures	
35	4.29[b]	64.8		
36	4.12[b]	63.8	Cγ in sinapyl/coniferyl/*p*-coumaryl alcohol end-groups	
37	4.22[b]	63.4		
38	4.05[b]	63.2		
28	3.69	56.2	$-OCH_3$ in syringyl and guaiacyl units	2.87

n.a. stands for "not assigned".

[a] Integral value for structural moieties expressed per one aromatic ring. The integral between 162–102 ppm was set as the reference, assuming that it represents 6.12 aromatic carbons (all aromatic C + a contribution of 0.12 from the unsaturated side chains of coumaric and coniferic groups).

[b] Protons referred to CH2 in the HSQC spectrum.

CH_γ in phenylcoumarans. These substructures were connected through ester or ether linkages with reactive monolignols such as ferulic and *p*-coumaric acids (with notably typical peaks in the range from δ_C/δ_H 115–118/6.66–6.92). The signals from δ_C/δ_H 62/3.43 to 4.05 was attributed to CH_γ in cinnamyl alcohol end-groups. Interestingly also, the HSQC spectrum of AL clearly showed specific carbohydrates cross-signals in the range δ_C/δ_H 70–85/3.0–4.5, indicating that the ammonia pre-treated lignin sample was "contaminated" by residual polysaccharides. The main cross-signals assigned in HSQC spectra of ammonia lignin are listed in Table 3.

Table 5

Main regions in the quantitative ^{13}C NMR spectra of formic/acetic acid lignins (FAL-107 and FAL-80) and ammonia lignin (AL) from *Miscanthus*. ^{13}C NMR spectra recorded in the presence of $Cr(acac)_3$ as the spin relaxing agent (0.01M).

δ ^{13}C (ppm)	Assignment	Value (per Ar) for AL	Value (per Ar) for FAL-80	Value (per Ar) for FAL-107
161–145	Aromatic C–O	1.84	2.13	3.06
140–126	Aromatic C–C	1.65	0.72	0.49
126–102	Aromatic C–H	2.45	2.76	2.69
90–58	Alk–O	2.81	1.77	1.10
90–77	Alk–O–Ar, α–O–Alk	0.37	0.08	0.06
77–64	γ–O–Alk, OH_{sec}	1.28	1.06	0.86
64–57	OH_{prim}	1.16	0.66	0.18

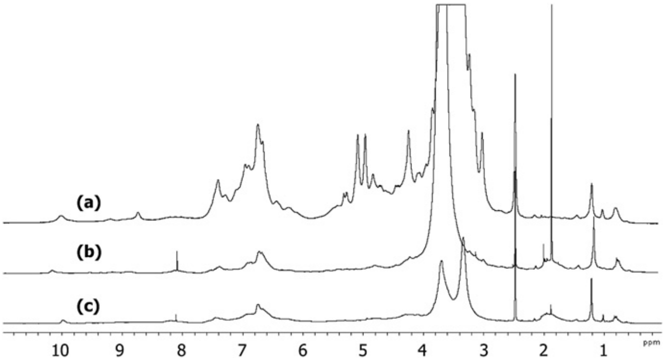

Fig. 3. ^1H NMR spectra of ammonia lignin AL (a) and formic/acetic acid lignins FAL-80 (b) and FAL-107 (c) recorded between δ 0.0 and 11.0 ppm in DMSO-d_6.

The aromatic and the side-chain regions of formic/acetic acid lignins (FAL-107 and FAL-80) are shown respectively in Fig. 4b–4c and Fig. 5b–5c, and the peaks assignment is proposed in Table 4.

The aromatic area was almost identical for both AL and formic/acetic acid lignins. However, examination of the side-chain area highlighted significant qualitative differences in the occurrence of inter-unit linkages. Although, for FAL-107, the CH_γ in β-5 substructures was identified at about δ_C/δ_H 65/4.20, there was no noticeable contribution of β–O-4′ structures. This observation reflected most probably a higher depolymerisation degree for this formic/acetic acid lignin than for ammonia lignin, with a higher preferential cleavage of β–O-4′ bonds under acid conditions. FAL-80 was considered as an intermediate situation between AL and FAL-107. Indeed, the HSQC spectrum revealed the presence of carbohydrates evidencing that the isolated FAL-80 was a short chain polysaccharides–lignin complex. Investigation of the type of linkages in the oxygenated side-chain area highlighted cross-signals at δ_C/δ_H 64–65/4.20–4.30 assigned to C_γ–H_γ correlation in β-5 substructures. Whereas β–O-4′ bonds were completely hydrolysed at 107 °C, HSQC analysis showed that these linkages (δ_C/δ_H 60.4/3.20–3.60) were partially preserved under milder pretreatment conditions.

The signal assignments proposed in Tables 3 and 4 were further confirmed by performing {^{13}C–^1H} HSQC analyses on acetylated lignin samples [15]. The major differences were observed in the oxygenated side-chain area of the spectrum, as illustrated in Fig. 6. After acetylation, as represented on the HSQC spectrum of AL, the cross-signals at δ_C/δ_H 74.2/5.96 and 63.8/4.18–3.75 (Fig. 6a) were correlated to acetylations at C_α and C_γ positions respectively in β–O-4′ substructures, while peaks at about δ_C/δ_H 67.4/3.64 were assigned to acetylated C_γ–H_γ correlation in β-5 phenylcoumaran linkages. In the HSQC spectrum of FAL-107, we observed nearly complete disappearance of signals corresponding to C_γ-H_γ correlation in β–O-4′ lignin structures, validating thus that acid organosolv fractionation induced β–O-4′ cleavage.

Linkages in AL and FAL-107 structures are depicted in Fig. 7.

3.6. *Quantitative lignin characterisation by ^{13}C NMR spectroscopy*

The structural elucidation done, it was possible to estimate the content of characteristic structures present in a lignin sample using quantitative ^{13}C NMR technique. For this purpose, $Cr(acac)_3$ was added as the spin relaxing agent and allowed a significant reduction of relaxation time of all nuclei [27]. Practically, a 4-fold decrease in the experimental acquisition time was encountered to obtain spectra of good quality.

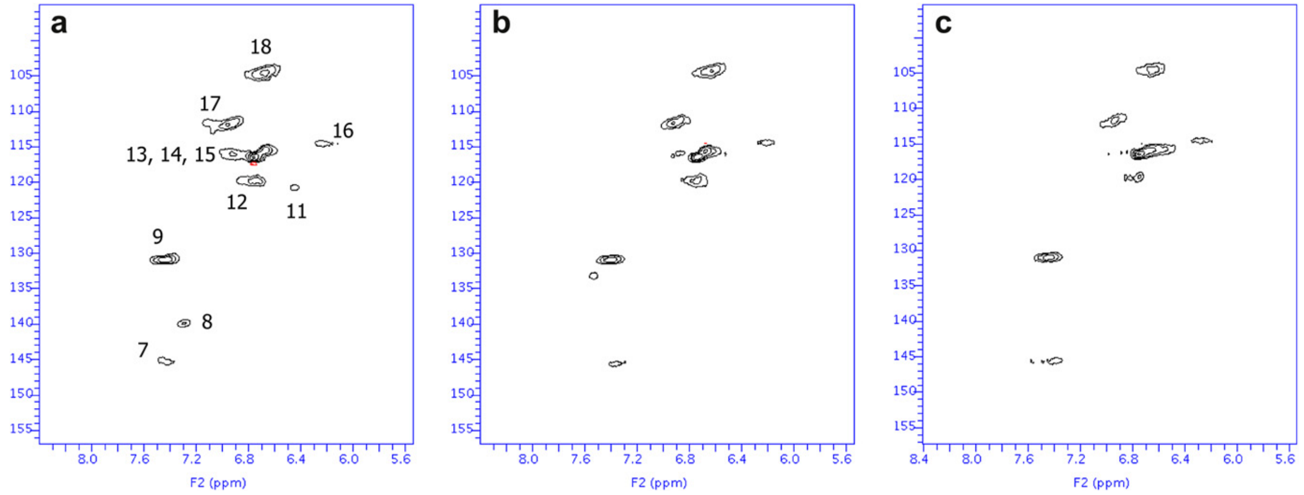

Fig. 4. Expanded aromatic region of HSQC spectra of ammonia lignin AL (a) and formic/acetic acid lignins FAL-80 (b) and FAL-107 (c). Peak labels are referred to Tables 3–4.

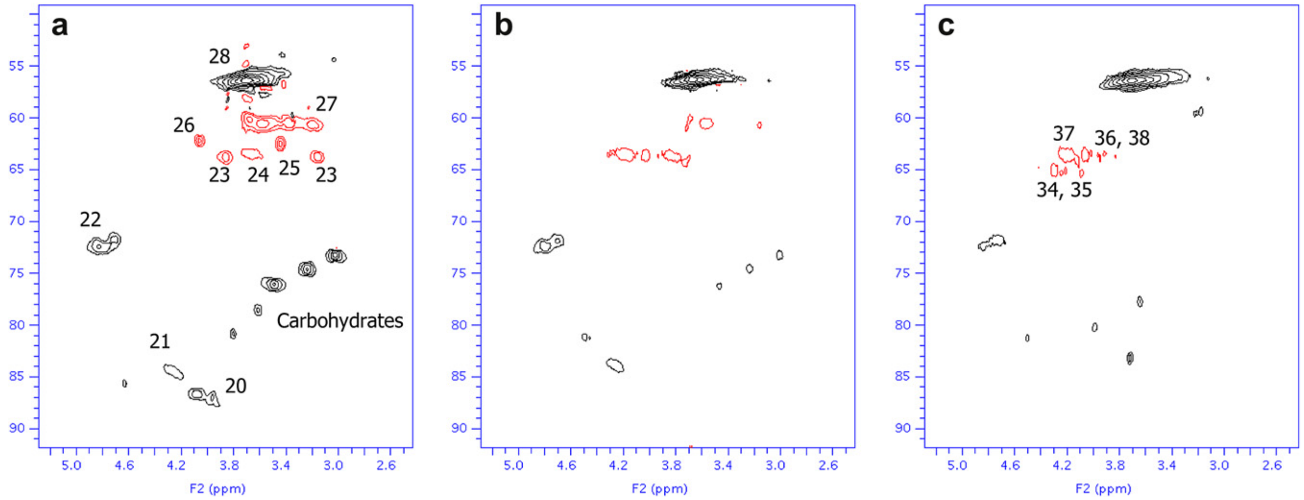

Fig. 5. Expanded oxygenated aliphatic region of HSQC spectra of ammonia lignin (a) and formic/acetic acid lignins FAL-80 (b) and FAL-107 (c). Peak labels are referred to Tables 3–4. By convention, peaks in red are associated with CH_2. (For interpretation of the references to colour in this figure legend, the reader is referred to the web version of this article.)

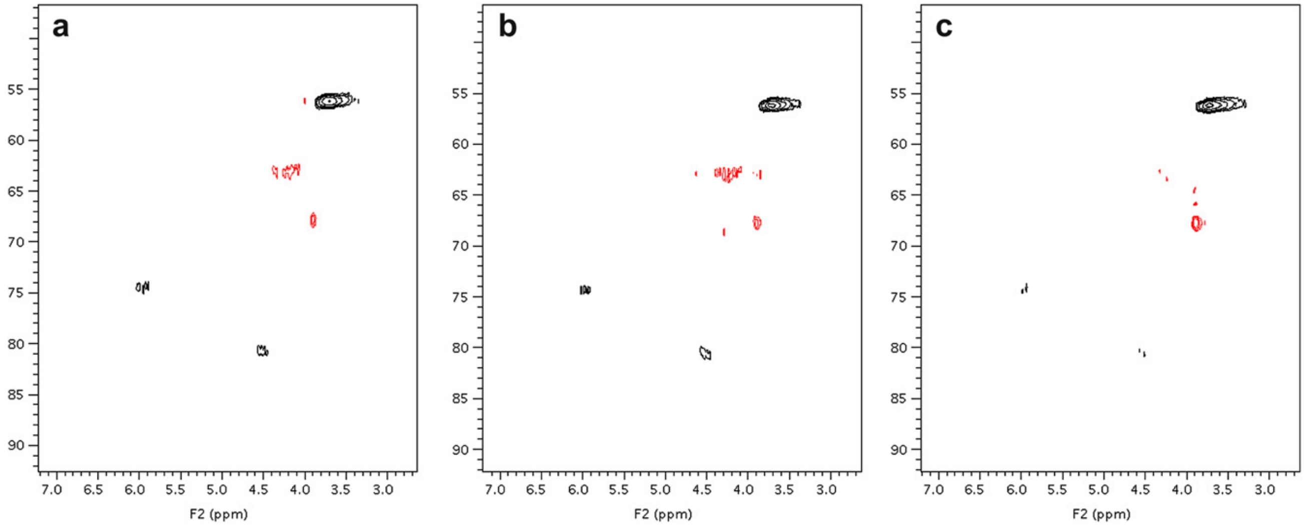

Fig. 6. Expanded oxygenated aliphatic region of HSQC spectra of acetylated ammonia lignin (a) and acetylated formic/acetic acid lignins FAL-80 (b) and FAL-107 (c). By convention, peaks in red are associated with CH_2. (For interpretation of the references to colour in this figure legend, the reader is referred to the web version of this article.)

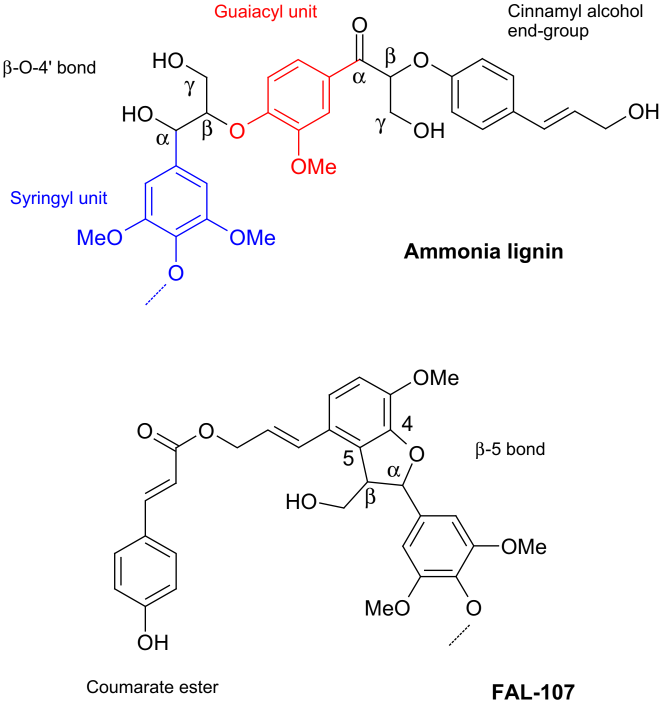

Fig. 7. Linkages in ammonia lignin (AL) and formic/acetic acid lignin (FAL-107) structures.

For the estimation of different lignin moieties content from ^{13}C NMR data, the integral of the δ_C 102–162 ppm region was set as a reference, assuming that it represented six aromatic carbon and 0.12 vinyl carbons. As a consequence, the integral value divided by 6.12 was equivalent to one aromatic ring (Ar) [28]. It assumed that the integral value estimated for other structural features was expressed per one aromatic ring.

^{13}C NMR spectra of AL and FAL-107 are respectively proposed in Figs. 8 and 9. The region between δ_C 100–165 ppm corresponded to aromatic carbons from monolignols structural units. As previously published, guaiacyl units (G) produced notably characteristic signals at δ_C 150.0 (C_3 etherified), 147.5 (C_4 etherified) and 119.5 ppm (C_6) [12]. Syringyl units (S) displayed peaks at δ_C 152–153 (C_3 and C_5 etherified) and 103–104 ppm (C_2 and C_6). *p*-Hydroxyphenyl units (H) appeared with very weak signals at about δ_C 128 ppm.

Differences in shape could be observed at δ_C ranging from 160 to 175 ppm. These signals corresponded to *p*-coumaric acid esters predominantly found in FAL-107. The particular peak at δ_C 170 ppm was tentatively assigned to acetate groups, arising from residual trace of acetic acid employed during the pretreatment protocol.

In the aliphatic region (60–90 ppm), ammonia lignin displayed a well-resolved spectrum, with peaks characteristic of C_α, C_β and C_γ in β–O-4′ linkages, rationalising that the alkali process did not degrade the lignin macromolecule to a significant extend [12]. At the opposite, very weak signals were recorded in the same chemical shift area for FAL-107. This observation corroborated previous works describing the dissolution of lignin by predominant β–O-4′ linkages cleavage under acid conditions [29].

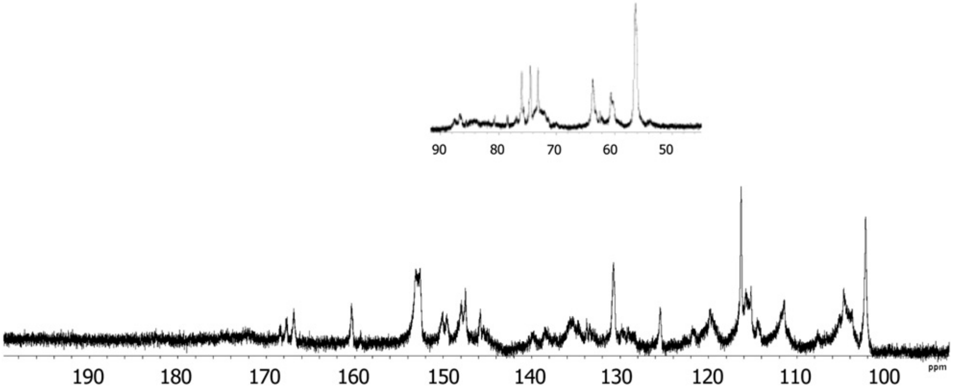

Fig. 8. ^{13}C NMR spectrum of ammonia lignin recorded with $Cr(acac)_3$ as the spin relaxing agent.

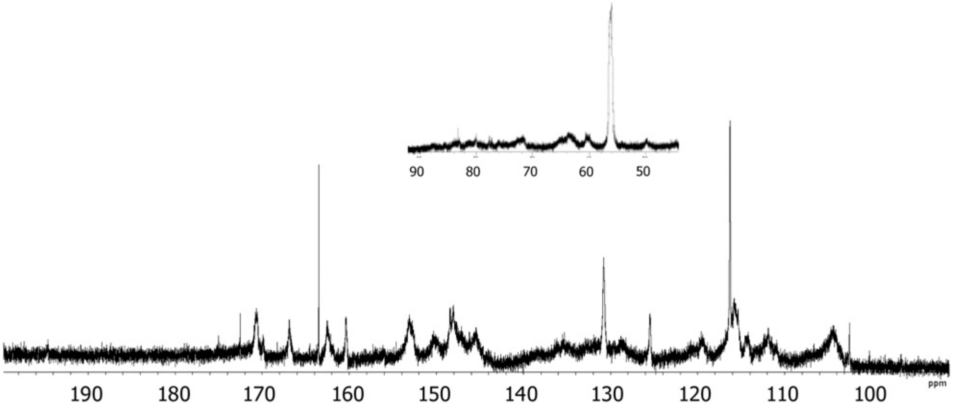

Fig. 9. ^{13}C NMR spectrum of formic/acetic acid lignin (FAL-107) recorded with $Cr(acac)_3$ as the spin relaxing agent.

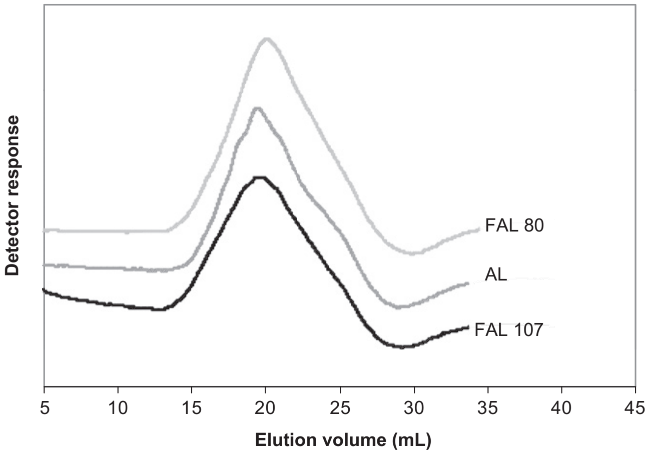

Fig. 10. Gel permeation chromatograms of acetylated formic/acetic acid lignins FAL-80, FAL-107, and ammonia lignin AL isolated from *Miscanthus x giganteus*.

Quantification of signals between 58 and 90 ppm, relative to Alk-O contributions, was of about 2.81/Ar for ammonia lignin and quite lower (1.10/Ar) for formic/acetic acid lignin as illustrated in Table 5. In the same vein, calculation on the basis of integration of total amount of Alk–O–Ar and α–O–Alk contribution was of 0.37/Ar and 0.06/Ar for respectively ammonia and formic/acetic acid lignin. In complement, the number of condensed aromatic carbons ("aromatic C–C") decreased from 1.65/Ar for ammonia lignin to 0.72/Ar for FAL-80 and 0.49/Ar for FAL-107, confirming a progressive decrease in the degree of condensation for lignin obtained under the acid conditions used.

Examination of Table 5 demonstrated thus a logical evolution of all clusters composition. FAL-107 displayed the lowest primary hydroxyls content (0.18/Ar *vs*. 1.16/Ar for AL), whereas this content was quite intermediate for FAL-80 (about 0.66/Ar). In parallel, the aromatic C–O linkages content shifted from 3.06/Ar for FAL-107 to 2.13/Ar for FAL-80 and 1.84/Ar for AL. This observation implied that organosolv acid processes induced a large reduction of aliphatic hydroxyl groups together with a significant increase of free phenolic hydroxyls [15].

3.7. Molecular weight

The weight average (M_w) of acetylated lignins was analysed from the GPC chromatograms (Fig. 10). FAL-107 had a M_w 2760 g mol^{-1}superior to FAL-80 M_w 2350 g mol^{-1}. AL resulted in the major M_w 3140 g mol^{-1}.

The M_w of FAL-107 was expected to decrease as a result of the important cleavage of β–O-4′ linkages as a result of the acid pretreatment in harsh conditions, but this was not the case. The cleavage of β–O-4′ linkages obtained under the conditions used in this pretreatment could have been accompanied by a repolymerisation resulting in an increase in molecular weight.

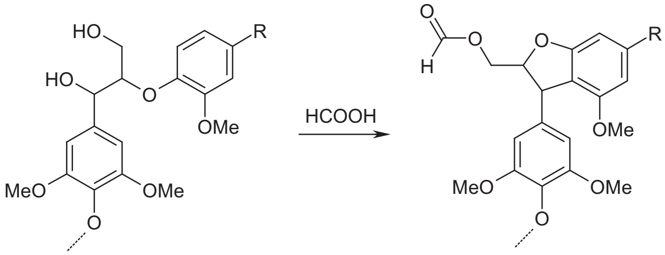

Fig. 12. Intramolecular condensation of lignin compounds in formic acid conditions.

Two predominant reactions occur under acidic conditions: lignin fragmentation by acidolysis of β–O-4′ linkages (Fig. 11) and polymerization by acid-catalyzed condensation between the aromatic C_6 or C_5 and a carbonium ion [30]. The results obtained in the NMR confirmed the former reaction. In fact β–O-4′ bonds were completely cleaved at 107 °C. Nevertheless, the second reaction was not detected because the aromatic C–C did not increase for the FAL-107, indicating a progressive decrease in the degree of polymerization.

Several hypothesis were thus formulated at this stage. The first one could originate from a recondensation of FAL-107 under acidic conditions, not via formation of aromatic C–C bonds, but through new aromatic C–O linkages (*i.e.* formation of *p*-coumaric acid esters as observed by ^{13}C NMR in Table 4 or via specific coupling as mentioned by Grabber [31]). Intramolecular condensation could also occur in formic acid conditions, leading to the formation of new structures as illustrated in Fig. 12 [32].

Secondly, it should be mentioned that weight averages (M_w) were estimated reasoning on volumetric weights. This implies that neither the conformation of lignin samples in THF nor interactions (hydrogen bonds) between molecules were considered.

3.8. Antioxidant activity

The RSI values of FAL-107, FAL-80 and AL were 0.40, 0.25 and 0.24 respectively. Higher antioxidant activity results in higher RSI value. It can be found that FAL-107 had a much higher antioxidant activity than the others lignins. According to Dizhbite et al. [10], RSI was positively correlated to phenolic hydroxyl group and had no effect with aliphatic hydroxyl group in real lignins.

According to our results, the organosolv acid processes induced a large reduction of aliphatic hydroxyl groups together with a significant increase of free phenolic hydroxyls, explaining the greater antioxidant activity of FAL-107 (Fig. 11). In addition, FAL-80 and AL radical scavenging activity could be negatively affected by the presence of non-lignin components as hemicellulose by hydrogen bonding with lignin phenolic groups [10,33].

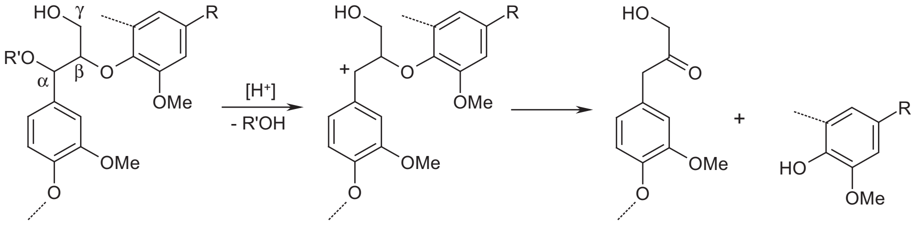

Fig. 11. Cleavage of β–O-4′ linkages in formic/acetic acid lignin (FAL-107) and liberation of free phenolic groups responsible of the antioxidant activity [30].

4. Conclusions

In the acid pretreatment in harsh conditions (FAL-107) depolymerisation and repolymerisation took place. Cleavage of β–O-4′ bonds and aromatic C–C were the major mechanisms of lignin breakdown. Repolymerisation was thought to originate from formation of new ester substructures.

Under milder conditions (FAL-80) fewer β–O-4′ linkages were broken and repolymerisation took place to a lesser extent. Ammonia lignin was “contaminated” by residual polysaccharides but was not degraded to a significant extent.

Despite the repolymerisation of FAL-107 significant phenolic hydroxyls remained free, explaining the greater antioxidant activity.

Acknowledgements

This study was financially supported by the Walloon Region (TECHNOSE project number 716757). Ms. Virginie Byttebier is acknowledged for excellent assistance. Mr. Mario Aguedo is acknowledged for his help in molecular weight analysis. Mrs. Lynn Doran is acknowledged for the thermogravimetric analysis.

References

[1] Johnson DK, Chornet E, Zmierczak W, Shabtai J. Conversion of lignin into a hydrocarbon product for blending with gasoline. Fuel Chem Division Preprints 2002;47(1):380–1.
[2] Buranov AU, Mazza G. Lignin in straw of herbaceous crops. Ind Crops Prod 2008;28:237–59.
[3] Lewis NG, Yamamoto E. Lignin: occurrence, biogenesis and biodegradation. Annu Rev Plant Mol Biol 1990;41:455–96.
[4] Chakar FS, Ragauskas AJ. Review of current and future softwood kraft lignin process chemistry. Ind Crops Prod 2004;20:131–41.
[5] Freudenberg K, Grion G. Contribution to the mechanism of formation of lignin and of the lignin-carbohydrate bond. Chem Ber 1959;92:1355–63.
[6] Freudenberg K, Harkin JM. Models for the linkages of lignin to carbohydrates. Chem Ber 1960;93:2814–9.
[7] Kosikova B, Joniak D, Skamla J. Lignin-carbohydrate bonds in beech wood. Cell Chem Technol 1972;6:579–88.
[8] Gosselink RJA, de Jong E, Guran B, Abächerli A. Co-ordination network for lignin – standardisation, production and applications adapted to market requirements (EUROLIGNIN). Ind Crops Prod 2004;20:121–9.
[9] Zakzeski J, Bruijnincx PCA, Jongerius AL, Weckhuysen BM. The catalytic valorization of lignin for the production of renewable chemicals. Chem Rev 2010;110:3552–99.
[10] Dizhbite T, Telysheva G, Jurkjane V, Viesturs U. Characterization of the radical scavenging activity of lignins-natural antioxidants. Bioresour Technol 2004; 95:309–17.
[11] Murnen HK, Balan V, Chundawat S, Bals B, da Costa Sousa L, Dale BE. Optimization of ammonia fiber expansion (AFEX) pretreatment and enzymatic hydrolysis of *Miscanthus x giganteus* to fermentable sugars. Biotechnol Prog 2007;23:846–50.
[12] El Hage R, Brosse N, Chrusciel L, Sanchez C, Sannigrahi P, Ragauskas A. Characterization of milled wood lignin and ethanol organosolv lignin from *miscanthus*. Polym Degrad Stab 2009;94(10):1632–8.
[13] El Hage R, Brosse N, Sannigrahi P, Ragauskas A. Effects of process severity on the chemical structure of *Miscanthus* ethanol organosolv lignin. Polym Degrad Stab 2010;95(6):997–1003.
[14] Le Ngoc Huyen T, Rémond C, Dheilly RM, Chabbert B. Effect of harvesting date on the composition and the saccharification of *Miscanthus x giganteus*. Bioresour Technol 2010;101:8224–31.
[15] Villaverde JJ, Li J, Ek M, Ligero P, de Vega A. Native lignin structure of *Miscanthus x giganteus* and its changes during acetic and formic acid fractionation. J Agric Food Chem 2009;57:6262–70.
[16] Lam HQ, Le Bigot Y, Delmas M, Avignon G. A new procedure for the destructuring of vegetable matter at atmospheric pressure by a catalyst/ solvent system of formic acid/ acetic acid. Applied to the pulping of triticale straw. Ind Crop Prod 2001;4:139–44.
[17] Sluiter A, Hames B, Ruiz R, Scarlata C, Sluiter J, Templeton D, et al. Determination of structural carbohydrates and lignin in biomass. Golden, CO., USA: National Renewable Energy Laboratory; 2008. Laboratory Analytical Procedure.
[18] Blakeney AB, Harris PJ, Henry RJ, Stone BA. A simple and rapid preparation of alditol acetates for monosaccharides analysis. Carbohydr Res 1983;113: 291–9.
[19] Abdullah SS, Yusup S, Ahmad MM, Ramli A, Ismal L. Thermogravimetry study on pyrolysis of various lignocellulosic biomass for potential hydrogen production. Int J Chem Biol Eng 2010;3(3):137–41.
[20] Wu Y, Zhao Z, Li H, He F. Low temperature pyrolysis characteristics of major components of biomass. J Fuel Chem Technol 2009;37(4):427–32.
[21] Uslu A, Faaij APC, Bergman PCA. Pre-treatment technologies and their effect on international bioenergy supply chain logistics. Techno-economic evaluation of torrefaction, fast pyrolysis and pelletisation. Energy 2008;33:1206–23.
[22] Serrano L, Egües I, González Alriols M, Llano-Ponte R, Labidi J. Miscanthus sinensis fractionation by different reagents. Chem Eng J 2010;156(1):49–55.
[23] Sun RC, Tomkinson J, Bolton J. Effects of precipitation pH on the physicochemical properties of the lignins isolated from the black liquor of oil palm empty fruit bunch fibre pulping. Polym Deg Stab 1999;63(2):195–200.
[24] Ralph SA, Ralph J, Landucci LL. NMR Database of Lignin and Cell Wall Model Compounds. Available at, http://ars.usda.gov/Services/docs.htm?docid=10491; 2004.
[25] Capanema EA, Balakshin MY, Kadla JF. A comprehensive approach for quantitative lignin characterization by NMR spectroscopy. J Agric Food Chem 2004; 52:1850–60.
[26] Toledano A, Serrano L, Garcia A, Mondragon I, Labidi J. Comparative study of lignin fractionation by ultrafiltration and selective precipitation. Chem Eng J 2010;157(1):93–9.
[27] Xia Z, Akim LG, Argyropoulos DS. Quantitative 13C NMR analyses of lignins with internal standards. J Agric Food Chem 2001;49:3573–8.
[28] Chen CL. In: Lewis N, Sarkanen S, editors. Characterization of milled wood lignins and dehydrogenative polymerizates from monolignols by carbon-13 NMR spectroscopy, Lignin and Lignan Biosynthesis. Washington DC: American Chemical Society; 1998. p. 255–75. ACS Symposium Series 697.
[29] Pan XJ, Xie D, Yu RW, Lam D, Saddler JN. Pre-treatment of lodgepole pine killed by mountain pine beetle using the ethanol organosolv process: fractionation and process optimization. Ind Eng Chem Res 2007;46(8):2609–17.
[30] Li J, Henriksson G, Gellerstedt G. Lignin depolymerization/repolymerisation and its critical role for delignification of aspen wood by steam explosion. Bioresour Technol 2007;98:3061–8.
[31] Grabber JH. How do lignin composition, structure, and cross-linking affect degradability? A review of cell wall model studies. Crop Sci 2005;45:820–31.
[32] McDonough TJ. The chemistry of organosolv delignification. Tappi J 1993;76: 186–93.
[33] Garcia A, Toledano A, Andrés MA, Labidi J. Study of the antioxidant capacity of *Miscanthus sinensis* lignins. Proc Biochem 2010;45:935–40.